Surface Science 627 (2014) 42–48

Contents lists available at ScienceDirect

Surface Science

journal homepage: www.elsevier.com/locate/susc

Oxygen assisted H_2O dissociation on the Pt{110}(1 × 2) surface from first principles

Víctor A. Ranea [a,*], Eduardo E. Mola [a,b]

[a] CCT-La Plata-CONICET, Instituto de Investigaciones Fisicoquímicas Teóricas y Aplicadas (INIFTA), Facultad de Ciencias Exactas, Universidad Nacional de La Plata. Calle 64 y Diagonal 113, 1900 La Plata, Argentina

[b] Facultad de Química e Ingeniería Pontificia Universidad Católica Argentina, Av. Pellegrini 3314 CP 2000 Rosario, Argentina

ARTICLE INFO

Article history:
Received 26 December 2013
Accepted 7 April 2014
Available online 16 April 2014

Keywords:
Water molecule
Density functional calculations
Metal surface
Adsorption
Desorption
Dissociation

ABSTRACT

Water dissociation with and without oxygen coadsorption is investigated on the Pt{110}(1 × 2) surface at low coverage from first principles. Calculations indicate that desorption of the water molecule is likely to occur from the clean surface ahead of partial dissociation. The assistance of coadsorbed atomic O in the H_2O partial dissociation changes the picture. Several $H_2O + O \rightarrow OH + OH$ possible reactions (with no OH + H + O intermediate step) have been analyzed. The comparison between the activation energy for the mentioned reaction and the activation energy for H_2O desorption shows no *strong* preference for one reaction over the other one. These results predict that the partial dissociation of H_2O is a likely process if it is assisted by atomic O on the Pt{110}(1 × 2) surface. Dissociation and desorption of the H_2O molecule are competitive processes on the surface and is possible to predict a dynamic system.

1. Introduction

The interaction of water with surfaces has a paramount importance in topics of physics, chemistry and biology. The interaction of water (H_2O) with metal and metal oxide surfaces has been investigated using experimental and theoretical approaches [1–17]. Despite its catalytic properties, the Pt{110} surface is probably one of the platinum surfaces less studied (of the low index surfaces), see references [18–23] and references within. The {110} surface of platinum is one of the few surfaces (also Ir and Au) which spontaneously reconstructs to the (1 × 2) missing row reconstruction [24–27]. It is possible to differentiate three main *zones*: the *ridge*, the {111}-like facet and the *valley* with different reactivities, Fig. 1. Unlike the fcc{111} and the fcc{100} surfaces, most of the surface atoms have different coordination number in this reconstructed surface. In the present report, the adsorption of H_2O, OH, O and H is studied on the three mentioned *zones*. On the Pt{111} surface, the adsorption of water has been studied at different coverages [7–11,28,29]. In the low coverage regime, the adsorption is via the oxygen atom monocoordinated to a platinum atom of the surface. The plane of the water molecule is nearly parallel to the surface [9]. Similar adsorption configurations are found in the present report on the {110} face. It is also known that the Pt{001} surface reconstructs to a hex-phase ([30] and references within). The adsorption of water on the {110} surface of platinum has been previously investigated using experimental and theoretical techniques [14,15,31–33] at a higher coverage.

About two decades ago, Fusy and Ducros applied thermal desorption spectroscopy, ultraviolet electron spectroscopy, photoemission of adsorbed xenon and electron stimulated desorption ion angular distribution to study the adsorption of H_2O on Pt{110}–(1 × 2) [14]. At 100 K they found that water adsorbs molecularly as small clusters. At 300 K, water is partially dissociated to hydroxyl radicals when O is preadsorbed on the surface.

Recently, Shavorskiy and coworkers [15] applied temperature-programmed desorption (TPD) and X-ray photoelectron spectroscopy (XPS) to study the interaction of water and coadsorbed O with the missing-row reconstructed Pt{110}(1 × 2) surface. They found that in the absence of oxygen on the surface, the water stays intact at all temperatures between 140 and 175 K forming a strongly bound layer of 2 ML coverage. The oxygen coadsorption below saturation leads to the formation of OH. For small exposures of water a single peak appears in the TPD spectra. The maximum of the water desorption rate is at 178 K. The peak temperature shifts to 175 K when the water coverage increases to less than 1 ML coverage. Ren and Meng [33] applied density functional theory to study trends in the adsorption energy of water on the {110} surface of Cu, Ag, Au, Pd and Pt. They found that molecular adsorption on the *top* site, is preferred to dissociative adsorption on the Pt{110} surface by 0.192 eV (adsorption energy, $E_a^{H_2O} = -0.423$ and $E_a^{OH+H} = -0.231$ eV) at low coverage.

* Corresponding author.
E-mail address: vranea@inifta.unlp.edu.ar (V.A. Ranea).

http://dx.doi.org/10.1016/j.susc.2014.04.005
0039-6028/

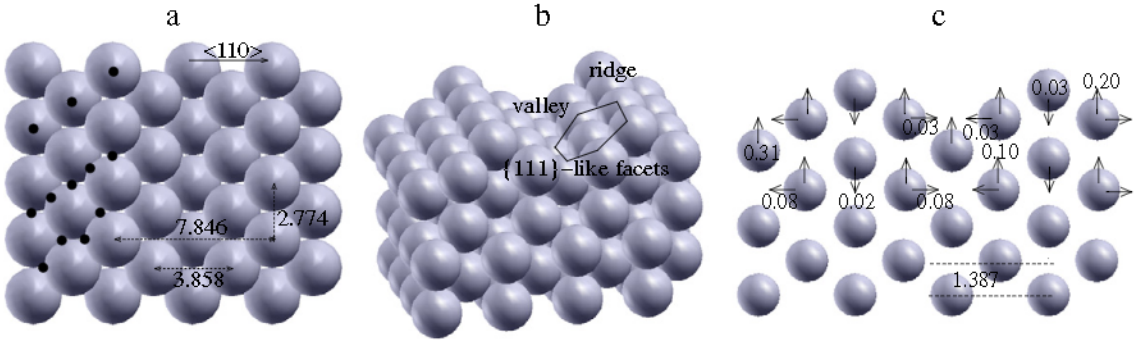

Fig. 1. Balls represent platinum atoms of the clean Pt{110}–(1 × 2) surface. Black dots in (a) (top view) indicate the initially studied adsorption sites. On (b) the *{111}-like* facets, the *ridge* and the *valley* are shown. The arrows in (c) show the direction of displacement of the atoms (qualitatively). Also the ideal interlayer spacing is shown. All the distances and displacements are in Å.

In the present manuscript we use density functional theory (DFT) and nudged elastic band (NEB) methodologies to investigate the effect of the atomic oxygen coadsorption in the H_2O partial dissociation at low coverage of water on the Pt{110} surface. Similar works have been performed on the Pt{111} surface at a higher coverage of water and oxygen [7,34–36].

The clean reconstructed {110}–(1 × 2) surface is first studied, then the adsorption of the involved species: H_2O, OH, O, and H. Partial dissociation of the H_2O molecule is investigated with and without the presence of coadsorbed atomic oxygen. The energy difference between molecular adsorption and dissociative adsorption is 0.45 eV, at least, and the activation energy for dissociation is calculated to be 0.73 eV when H_2O is isolated on the surface (water coverage = 1/8 ML). If atomic oxygen is present on the surface but does not take part of the partial dissociation reaction the energy difference between molecular adsorption and dissociative adsorption does not decrease. The results of the calculations using similar theoretical methods [7] on the {111} face show very similar energies for this process, endothermic process by 0.47 eV and an activation energy of 0.68 eV.

If atomic oxygen is present on the surface and takes part of the dissociation reaction $H_2O + O \rightarrow OH + OH$ with no intermediate steps (no OH + H + O on the surface) the energy difference between molecular and dissociative adsorption decreases markedly in the calculations reported here and on the Pt{111} surface [7]. Michaelides and Hu [7] used DFT methodologies to calculate the activation energy for this process on the {111} surface at a higher coverage of the adsorbates. They worked with a 0.25 ML coverage of water adsorbed on a p(2 × 2) surface with oxygen adsorbed also at 0.25 ML coverage. The final configuration was OH adsorbed at 0.5 ML coverage. The energies they found are smaller than the ones reported here. The reaction process is endothermic by 0.2 eV and the activation energy is 0.33 eV. The calculations reported here and those reported in Ref. [7] do not include the van der Waals interactions [28].

In the present manuscript, activation energies are calculated for the mentioned reaction and compared with the activation energies calculated for the coadsorbed H_2O desorption. H_2O dissociation is a likely process if the coadsorbed atomic oxygen assists the mentioned dissociation. This process is competitive with the coadsorbed H_2O desorption from the surface. Desorption and dissociation of the H_2O molecule are competitive processes on the mentioned surface and is possible to predict a dynamic system.

2. Theoretical approach

First-principles total energy calculations were performed using DFT to investigate the adsorption and dissociation of H_2O on the Pt {110}(1 × 2) surface as implemented in the Vienna Ab initio Simulation Package (VASP) [37,38] code. The Kohn–Sham equations were solved using projector augmented wave (PAW) method [39,40] and a plane-wave basis set including plane waves up to 400 eV. Electron exchange and correlation energies were calculated within the generalized gradient approximation (GGA) in the Perdew–Wang form [41]. Convergence is considered achieved when the forces on the ions are less than 0.03 eV/Å. Periodic boundary conditions are applied in the three perpendicular directions. Spin polarized calculations were performed when isolated OH or O or H species were the adsorbate. The Climbing Image Nudged Elastic Band (CI-NEB) method [42] was used to estimate the activation energy for water dissociation. Converged H_2O + O and OH + OH states were set as initial and final states and one image was used in the estimation. The atomic structure and the total energy of the image in each CI-NEB calculation were considered converged when the forces on the ions were less than 0.05 eV/Å. We are aware that sometimes more images are needed in order to have a precise description of the potential energy pathway. The only image used in the estimation was forced to the maximum in the potential energy path between the initial and final states. The estimated values seem to be consistent with previous results on Pt{111} [7].

The system (adsorbate + substrate) is modeled by a rectangular based supercell with lattice constants: $a = 7.8462$, $b = 11.0962$ and $c = 19.4184$ Å [43]. The surface is modeled by a seven-layer thick slab separated by more than 11 Å vacuum region, enough to avoid interactions between slabs [44]. The four external atomic layers were allowed to relax, together with the adsorbate, and the three bottom ones were kept fixed at their ideal bulk positions. A 15 Å side cubic supercell was used to calculate the H_2O, OH, H_2 and O_2 isolated species energies and structures. The first Brillouin zone was sampled with a (3 × 2 × 1) Γ centered mesh and only the Γ point was used for the cubic supercell.

The adsorption energy of the adsorbate is calculated as:

$$E_{ad} - E(\text{adsorbate}/srf) - E(\text{adsorbate}) - E(srf). \quad (1)$$

The first term of Eq. (1) is the energy of the optimized configuration of the adsorbate on the clean relaxed surface. The second term of Eq. (1) is the gas phase energy of the isolated adsorbate. When the *adsorbate* is hydrogen (or oxygen) $E(\text{hydrogen}) = E(H_2)/2$ (or $E(\text{oxygen}) = E(O_2)/2$), i. e., with respect to half of the energy in the gas phase of H_2 (O_2). The third term of Eq. (1) is the energy of the clean optimized surface. With this definition, negative values of E_{ad} are for stable configurations.

3. Results and discussions

3.1. Clean Pt{110} surface

The clean Pt{110} surface spontaneously reconstructs to the (1 × 2) missing row reconstruction [24–27]. DFT pseudopotential calculations showed that the {110} surface is 0.10 eV per (1 × 2) cell more stable than the (1 × 1) surface [44]. The model was proposed to describe the

(1×2) periodicity observed in the LEED pattern of the bare Ir{110} surface [26]. It consists of a {110} surface in which every other row in the <110> direction has been removed, as shown in Fig. 1. Removal of the rows produces ribbons of {*111*}-*like* facets across the surface, shown in Fig. 1b. The formation of these *stable* {*111*}-*like* facets has been cited as the driving force for the missing row reconstruction [30]. Fig. 1 shows the calculated displacement of the atoms of the four external layers, the arrows are to guide qualitatively the eye. The first interlayer spacing undergoes a contraction of ≈17% with respect to the ideal spacing, 1.387 Å, in agreement with experimental and theoretical results [44–49]. This contraction is a combination of an inward relaxation of the first layer and an outward relaxation of the second external layer, see Fig. 1. The atoms of the second layer also undergo small lateral shifts of 0.03 Å. The *exposed* Pt atoms of the third external layer undergo an outward relaxation of ≈0.31 Å while the Pt atoms underneath the first layer, a small inward relaxation of ≈0.02 Å. There is no lateral displacement of the atoms of this layer. With the exception of the vertical displacement of the atoms of the second layer, the displacement of the atoms of the three external layers is in a qualitative agreement with those calculated for Au{110}(1×2) [50]. The Pt atoms of the fourth external layer undergo similar qualitative displacement as the atoms of the second external layer.

3.2. Adsorption of the species: H_2O, OH, O and H

Adsorption of each individual species (H_2O, OH, O and H) has been investigated on twelve initial sites on the Pt{110}(1×2) surface. The initial sites have been marked with dots on the Fig. 1a.

3.2.1. H_2O adsorption

The molecular plane was initially set parallel to the surface plane. The O of the H_2O molecule was set on the studied sites (marked with dots on Fig. 1a) and two configurations were initially tested for each adsorption site: one OH pointing toward to the *ridge* or toward to the *valley*.

Four different adsorption configurations were found stable for the H_2O molecule. In the most stable configuration, the molecule is monocoordinated to a Pt atom of the *ridge* via the O atom with a calculated adsorption energy of −0.38 eV, as shown in the Fig. 2a. This adsorption energy agrees well with previous DFT calculations on the {110} [33] and {111} [7,9,51] surfaces of platinum, although the interaction is a bit stronger on the {110} surface. The molecular plane is nearly parallel to the surface plane as long as the molecule is not shifted from the *ridge*; otherwise the molecular plane tends to be nearly parallel to the {*111*}-*like* facet when the molecule is slightly shifted outside the *ridge* toward the valley, but still bound to one Pt atom of the *ridge*. The interaction of the H_2O molecule with one Pt atom of the *ridge* does not modify the position of the Pt atom neither of its neighbors. This is a different consequence from that one on fcc{111} surfaces where the top metal atom is pulled out when H_2O interaction takes place [9].

On the {*111*}-*like* facet the interaction is also via the oxygen atom with one Pt atom of the second external layer, as shown in Fig. 2b and c. The molecular plane is nearly parallel to the {*111*}-*like* facet. This adsorption configuration seems to be similar to the general model of H_2O adsorption on the {111} surface of metals [7,9,51–53]. On the Pt{110} surface, the rotational symmetry around the O–Pt axis found on {111} metal surfaces [9] is broken due to the neighbor *ridge* and *valley*. The adsorption energies are −0.29 and −0.15 eV whether one of the OH points toward to the *valley* or toward to the *ridge*, respectively; as shown in Fig. 2b and c. In these three adsorption configurations, the interaction between the water molecule and the surface resembles the interaction between the water molecule and the {111} surface of Pt and other transition metals [9,52,53]; also between the water molecule and the Al{100} [54] or the Al{111} [53] surfaces. The adsorption of the H_2O molecule on transition metal surfaces is due to the interaction of the $1b_1$ (mainly) and the $3a_1$ molecular orbitals with the wave functions of the surface [9,52]. A comparison between Fig. 2b and c shows that in Fig. 2b one of the H ends ('positive ends') of the H_2O molecule is pointing toward the *valley* where there is a *high* 'negative charge density' due to the Smoluchowski effect [55]. This attractive electrostatic interaction is probably one of the reasons of the 0.14 eV difference in the adsorption energy between these two configurations. Michaelides and coworkers [28] performed a series of DFT calculations for water adsorption on several metal surfaces, mainly fcc{111} (Al, Ru, Rh, Pd, Pt and noble metals) with and without the van der Waals interactions. A comparison between revPBE and revPBE-vdW is that the last one not always enhances the adsorption energy given by the revPBE. However, for Pt{111} the interaction with the water molecule is stronger when the vdW interactions are included in the calculations. On the {110} surface, it is expected that the adsorption energies are going to be higher when the vdW interactions are included, at least for the configurations described so far.

On the *valley*, the interaction of the H_2O molecule with the surface is less exothermic ($E_{ad}=-0.15$ eV) and it is via the H atoms with the oxygen atom away from the surface. This adsorption configuration seems to be due to a pure electrostatic interaction between the positive ends (hydrogens) of the water molecule and "the most negative region" of the surface.

3.2.2. OH adsorption

The OH fragment was initially set in three different configurations on the studied sites marked on Fig. 1a: parallel and perpendicular to the *ridge* (or to the *valley*), and perpendicular to the surface; in all the cases, bound via the oxygen atom.

Many adsorption configurations were found stable. We are going to focus on the most stable ones. The configuration in which the axis of the OH fragment is nearly parallel to the surface, pointing to the *valley* and bridging two Pt atoms of the *ridge* is the most exothermic one. The calculated adsorption energy is −2.77 eV. This adsorption configuration is in good agreement with previous DFT studies on the {111} surface of platinum [51]. In that article, Phatak and coworkers found that the most stable OH adsorption configurations on the Pt{111} surface is on the bridge and top sites with the OH axis tilted from the normal to the surface. Less exothermic is the OH adsorption monocoordinated to the

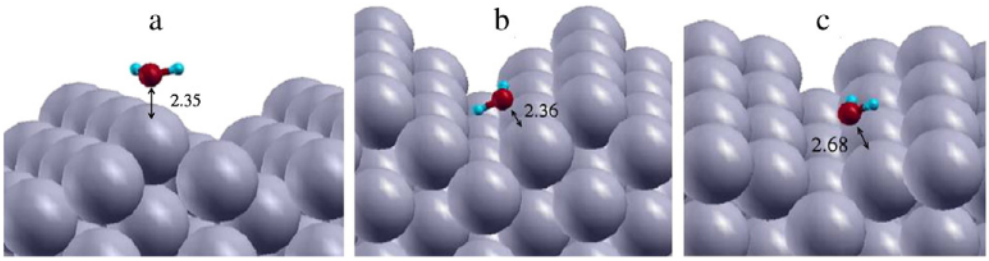

Fig. 2. Balls model for H_2O adsorption on the Pt{110}–(1×2) surface. (a) H_2O adsorption monocoordinated to the *ridge* with its plane nearly parallel to the {110} surface. H_2O adsorption on the {*111*}-*like* facet with its plane nearly parallel to the facet and one OH pointing to the *valley* in (b) and pointing to the *ridge* in (c). The distances are in Å. Big, medium and small balls stand for Pt, O and H atoms, respectively.

ridge via the oxygen atom; the OH fragment is also nearly parallel to the surface and the adsorption energy is in the *range* −2.69 (OH adsorbs parallel to the *ridge*) to −2.65 eV (OH adsorbs perpendicular to the *ridge*). The OH interaction with the {110} surface is stronger than that with the {111} surface [51] on these two (most stable) configurations.

As for the H_2O molecule, the *ridge* seems to be the most *attractive zone* for OH adsorption. This result is in a very good agreement with recent experimental results [15]. Other less exothermic adsorption configurations were found but they are not included in the present article.

3.2.3. O adsorption

Oxygen adsorbs molecularly or dissociatively on the Pt{110} surface at different substrate temperatures. Thermal desorption spectroscopy (TDS) and isotope tracer studies indicate that at temperatures below 180 K, oxygen adsorbs molecularly, whereas the dissociation of the molecules is in the temperature range of 180–220 K. Recombinant desorption of oxygen adatoms was observed above 650 K [56,57].

For atomic O adsorption, calculation shows many stable configurations. No energy difference (≤0.01 eV) was found when spin polarization is compared with non-spin polarization when adsorption takes place.

The bridge to two platinum atoms of the *ridge* is the most stable adsorption configuration for atomic oxygen with adsorption energy of −1.28 eV. The adsorption configuration in which the O atom is on the *hollow site* formed by two Pt atoms of the *ridge* and a Pt atom of the second layer (*fcc* hollow site) is only 0.04 eV less stable.

The calculated adsorption energy (−1.24 eV) is 0.06 eV less stable than the one calculated on the {111} surface [51]. This last adsorption site (*fcc* hollow site) is the most stable when the oxygen coverage increases [15]. As the coverage increases, the *fcc* hollow adsorption configuration accommodates two times the number of oxygen atoms adsorbed on the *bridge* site of the *ridge*.

As for OH, the *ridge* zone seems to be very active for atomic oxygen adsorption. These results are in agreement with recent TPD and XPS results [15]. These experimental results [15] indicate that OH and O adsorb on similar sites.

Less stable is the adsorption of O on the *hollow site* formed by one Pt of the *ridge* and two Pt atoms of the second layer (*hcp* hollow site). The calculated adsorption energy is −0.95 eV. A few less exothermic configurations were found stable.

3.2.4. H adsorption

Hydrogen adsorption is similar to O adsorption on the Pt{110} surface, although weaker. Hydrogen adsorption bridge to two Pt atoms of the *ridge* is the most stable with an adsorption energy of −0.48 eV. H adsorption on *top* of a Pt atom of the second layer is slightly less stable. The calculated adsorption energy is −0.45 eV. H adsorption on the *hollow site* formed by two Pt atoms of the *ridge* and one Pt atom of the second layer is a bit less favorable. The adsorption energy is −0.43 eV.

3.3. $H_2O \rightarrow OH + H$ partial dissociation

The most stable adsorption configuration for molecular H_2O is monocoordinated to a platinum atom of the *ridge*, as was stated above (Figs. 2a and 3a). After partial dissociation of the molecule, the fragments OH and H would remain coadsorbed on the surface near the initial H_2O adsorption site. Several coadsorption configurations of the fragments OH and H were optimized in some of their most stable configurations. Fig. 3b, c and d show OH adsorption in the *bridge* configuration of the *ridge* with the hydrogen adsorption on its three most stable adsorption configurations near the H_2O molecule original adsorption configuration. The energies of these three coadsorption configurations are in the range of only ≈0.10 eV. The coadsorption of the OH and H fragments is at least 0.45 eV less stable than the molecular adsorption in the most stable configuration, see Fig. 3 energy configurations *a* and *b*. Taking into account that molecular adsorption is an exothermic process with a calculated adsorption energy of −0.38 eV, the energy of the coadsorbed OH and H fragments is then ≈0.07 eV (−0.38 eV + 0.45 eV) over the energy level of reference. These values are taken with respect to the gas phase H_2O molecule and the clean optimized Pt{110} surface, as stated in the theoretical approach. The calculated repulsive interaction energy between OH and H coadsorbed fragments in the configuration shown in Fig. 3b is only 0.04 eV. This value is calculated with respect to adsorbed fragments separated by an infinite distance. This value of repulsive energy is small compared with the adsorption energy of the fragments and indicates that the OH and H fragments do not repel strongly from each other and makes the H_2O formation a likely process. Also, there would not be a strong driving force for the diffusion of the fragments at low temperature and low coverage due to this small value of repulsive energy. The activation energy for water dissociation is calculated to be 0.73 eV, this value is similar to that one calculated on the Pt{111} surface, 0.77 eV using similar theoretical frames [7].

The activation energy for molecular adsorption is 0 eV as Fig. 5 shows, see also reference [1] pg 254; and so the activation energy for water desorption is the absolute value of the adsorption energy. Because there is an energy difference of 0.35 eV between the activation energy for water desorption (0.38 eV) and the activation energy for water dissociation, the water molecular desorption to the gas phase is energetically preferred to the partial dissociation to OH + H on the surface, at the very low coverage we are working with. Following these results, the partial dissociation of the isolated H_2O molecule adsorbed on the surface is not favorable thermodynamically. Other less stable coadsorption configurations are shown in Fig. 3. Partial dissociation of the H_2O molecule seems to be an unlikely process (because it is not favorable thermodynamically) without the presence of coadsorbed molecules. This is in agreement with recent experimental results [15]. Shavorskiy and coworkers [15] found that direct dissociation reaction $H_2O \rightarrow OH + H$ does not occur on the clean surface.

How are the energy differences between molecular and dissociative adsorption affected after oxygen coadsorption (energy diagram in

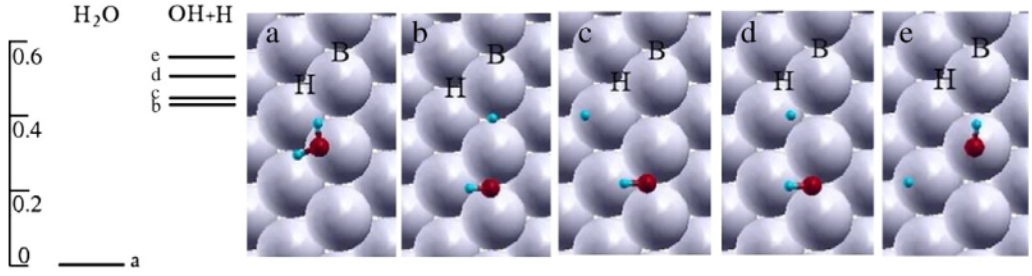

Fig. 3. (Left) energy diagram (relative energy) for the H_2O adsorption on the left column and the products (OH + H) on the column on the right. The adsorption energy of the H_2O molecule is 0.38 eV (a), whereas the lowest adsorption energy of the products is 0.07 eV (b). (right) Top views of all these configurations. The letters individualize the configurations with their energies. H_2O adsorption on the Pt{110} surface in (a). Panels (b), (c), (d) and (e) are models for OH + H coadsorption near the original H_2O adsorption site. *B* and *H* individualize sites where an extra oxygen atom coadsorbs. Big, medium and small balls stand for Pt, O and H atoms, respectively. The relative energies are in eV.

Fig. 3)? Atomic oxygen is coadsorbed on the sites marked as *B* and/or *H* in Fig. 3 with molecular and dissociated water. Oxygen coadsorption on the surface in a 1:1 relation with H_2O, at low coverage, does not decreases the energy difference between H_2O adsorption energy and the OH + H adsorption energy. Two cases were analyzed. First, oxygen coadsorption on the *bridge* site marked as *B* in Fig. 3 increases the energy difference between the energy of the molecular adsorption, configuration *a*, and the energy of dissociative adsorption by 0.13, 0.01, 0.12 and 0.04 eV, for configurations *b*, *c*, *d* and *e*, respectively and second, oxygen coadsorption on the site marked as *H* in Fig. 3, increases the energy difference by 0.09, 0.11, 0.11 and 0.04 eV from configuration *a* to configurations *b*, *c*, *d* and *e*, respectively. The energy difference was also tested for a 2:1 relation of O:H_2O for O coadsorption on the sites marked as *B* and *H* in Fig. 3. The energy difference increases by 0.16, 0.05, 0.14 and 0.07 eV from configuration *a* to configurations *b*, *c*, *d* and *e*, respectively.

As a conclusion of this subsection, we could indicate that the H_2O partial dissociation to OH and H on the Pt{110} surface is not, thermodynamically, a favorable process. At the very low coverage we are working, the water molecular desorption to the gas phase is energetically preferred to the partial dissociation to OH + H on the surface. This is in good agreement with previous experimental studies [58]. They found that water adsorbs intact at all temperatures on the Pt{110}(1×2) surface. The coadsorption of atomic O in relations 1:1 or 2:1 with H_2O does not decrease the relative energy between molecular adsorption and partially dissociated adsorption of OH and H. Partial dissociation of the H_2O molecule to OH + H on the Pt{110} surface is not a likely process even in the presence of coadsorbed O in the investigated relative concentrations, as long as the atomic oxygen does not assist the partial dissociation.

3.4. $H_2O + O \rightarrow OH + OH$ partial dissociation

The H_2O partial dissociation is investigated with the assistance of coadsorbed atomic oxygen on the Pt{110} surface. Several *initial* H_2O + O coadsorption configurations are investigated where both adsorbates are near enough to each other to produce a surface reaction. Both adsorbates are located in their most stable configurations. Only the most stable optimized configurations are shown in Fig. 4. Several OH + OH *final* configurations adsorbed near the original location of the H_2O + O species are investigated on the same Pt surface. Only the most stable optimized configurations are shown in Fig. 4. At this stage, there is no intermediate OH + H + O step on the surface. For different initial and final configurations, relative energies of the $H_2O + O \rightarrow OH + OH$ reaction are compared, also the activation energies are estimated and compared with the activation energy of the coadsorbed H_2O desorption.

Several $H_2O + O \rightarrow OH + OH$ reactions are possible without diffusion of the fragments. It is important to observe that all the energy differences between the most stable initial and final configurations are less than 0.25 eV regardless the reaction is endothermic or exothermic (see the left part of Fig. 4). This value of energy difference is smaller than the one calculated for partial dissociation of the H_2O molecule via the reaction $H_2O \rightarrow OH + H$ (at least 0.45 eV), as Fig. 3 shows. The energy diagram at the left part of Fig. 4 shows the lowest relative energies of several $H_2O + O$ and OH + OH configurations. Top views of them are shown at the right part of Fig. 4. Fig. 4a, b, c, d and e shows the $H_2O + O$ configurations and Fig. 4f, g and h, shows the OH + OH configurations.

The adsorption of a H_2O molecule is not an activated process, see Fig. 5, so the absolute value of the adsorption energy is equal to the activation energy for desorption of the isolated molecule on the surface, 0.38 eV. Whereas the activation energy for H_2O dissociation on this surface at the same coverage is 0.73 eV. The energy difference is then 0.35 eV, in the absence of coadsorbed atomic oxygen, thermodynamically the H_2O molecule is going to desorb from the surface, in line with experimental results [14,15]. The mentioned Fig. 5 also shows, for the O-H_2O coadsorption, that the activation energies for H_2O desorption from configurations *a*, *b*, *c* and *d* are the corresponding adsorption energies because the activation energy for adsorption seems to be 0 eV (see Fig. 5 squares, diamonds, triangles up and down, respectively, also Ref. [1], pg 254).

Configuration *a* is the most stable H_2O + O coadsorption, as can be seen from Fig. 4. Its adsorption energy is −1.65 eV with respect to the energy of the clean surface, the isolated water molecule and half of the energy of the isolated oxygen molecule. The estimated activation energies for dissociation to configurations *f* and *g* are 0.60 and 0.66 eV, respectively, as shown in Fig. 6 upper part left panel. These values are larger than the activation energy for H_2O desorption from configuration *a*, 0.38 eV (see Fig. 5, squares are the calculated energy data). The comparison shows that most of the H_2O molecules are likely to desorb from the surface rather than dissociate assisted by the coadsorbed oxygen atom. This energy value is very near to the activation energy for H_2O desorption from the clean surface (see Fig. 5, circles are the calculated energy data). This comparison indicates that the interaction energy between the fragments H_2O and O is near to 0 eV, in this configuration. Despite the fact that configuration *a* most likely occur at this coverage, the dissociation of the H_2O molecule is unlikely from the mentioned configuration due to the high activation energy ($\approx$ 0.6 eV) against the activation energy for desorption ($\approx$ 0.38 eV).

In configuration *b*, the fragments are more *in range* for reaction than in configuration *a* (the fragments are closer to each other than in configuration *a*). Configuration *b* is about 0.11 eV less stable than configuration *a* and so it is less likely to occur at the present coverage. A higher

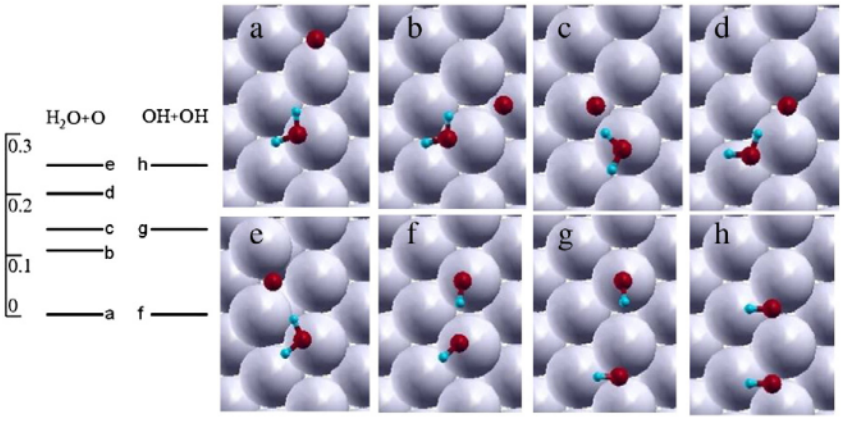

Fig. 4. (Left) energy diagram (relative energies) for the reactants (H_2O + O) on the left column and the products (OH + OH) on the column on the right. (right) Panels a, b, c, d and e show top views for H_2O + O coadsorption. Panels f, g and h show top views for OH + OH coadsorption. The relative energies are in eV. Big, medium and small balls stand for Pt, O and H atoms, respectively.

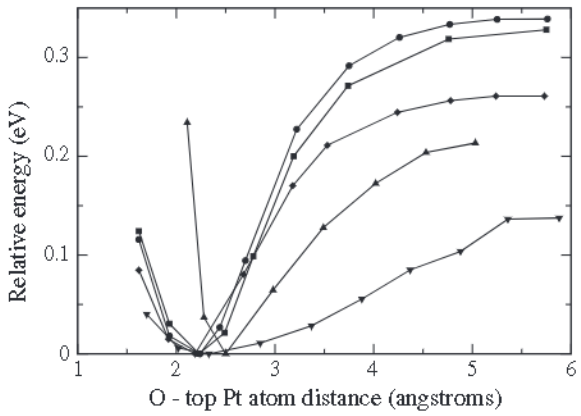

Fig. 5. Energy of the H_2O molecule (vertical axis, eV) as a function of the oxygen distance to the Pt{110} surface (horizontal axis, Å). The energy data are marked with circles for the clean surface (see Figs. 2a and 3a), squares, diamonds, triangles up and down for configurations *a*, *b*, *c* and *d*, respectively, in Fig. 4. For each energy value the *z* coordinate of the oxygen atom of the H_2O molecule is kept constant whereas their *x* and *y* coordinates are free to move. The hydrogen atoms are free to move. The activation energy for water adsorption seems to be 0 eV in every case whereas the activation energy for desorption is the adsorption energy (absolute value). The minimum of all the curves has been shifted to 0 eV. In the case of desorption from the clean surface (circles) the O-top Pt atom distances are (from left to right, in Å): 2.30, 2.32, 2.37, 2.53, 2.75, 3.31, 3.83, 4.33, 4.83, 5.31, 5.81. Near the surface there is an important lateral shift of the water molecule.

oxygen coverage will increase the probabilities of configurations *b* and *c*. As was already mentioned, when the oxygen coverage increases and oxygen is the only adsorbate on the surface, the most likely configuration is not the *bridge* but a *zig zag* configuration made of oxygen atoms adsorbed on three-fold sites by the *ridge*. The H_2O adsorption and desorption energy in the presence of the atomic oxygen is 0.31 eV (Fig. 5, upper part right panel, shows that there is no activation energy for adsorption; diamonds are calculated as energy data points). The activation energies for H_2O dissociation from configuration *b* to configurations *f* and *g* are 0.47 and 0.26 eV, respectively, as shown in Fig. 6. These values show that dissociation of the H_2O molecule is more likely from configuration *b* than from configuration *a* and from the isolated molecule adsorbed on this surface, see Fig. 5. From this coadsorption configuration, the dissociation (0.47 and 0.26 eV) and the desorption (0.31 eV) of the H_2O molecule are competitive processes.

Configuration *c* is 0.14 eV less stable than configuration *a*. The estimated activation energies for H_2O dissociation from configuration *c* to configurations *f* and *g* are 0.44 and 0.42 eV, respectively, see Fig. 6 bottom part left panel. These energies are a bit higher than the activation energy for H_2O desorption, 0.26 eV, see Fig. 5 triangles up are the calculated energy data points. From this configuration, dissociation (0.44 and 0.42 eV) and desorption (0.26 eV) are competitive processes although desorption seems to be a bit more likely.

Configuration *d* is less stable than configurations *a*, *b* and *c* (and less likely to occur) but dissociation of the H_2O molecule seems to be more likely to occur than from those configurations. Activation energies for dissociation of the H_2O molecule from configuration *d* to configurations *f* and *g* are 0.27 and 0.21 eV, respectively, see Fig. 6 bottom part right panel. Although the values of energy are smaller than the previous ones they are a bit larger than the activation energy for H_2O desorption, 0.18 eV, from this configuration, see Fig. 5 triangles down. From configuration *d*, dissociation (0.27 and 0.21 eV) and desorption (0.18 eV) of the H_2O molecule seem to be competitive processes under the studied coverage.

At the low coverage studied and at the H_2O:O relation of 1:1, the system seems to be very dynamic. One can add the energy difference

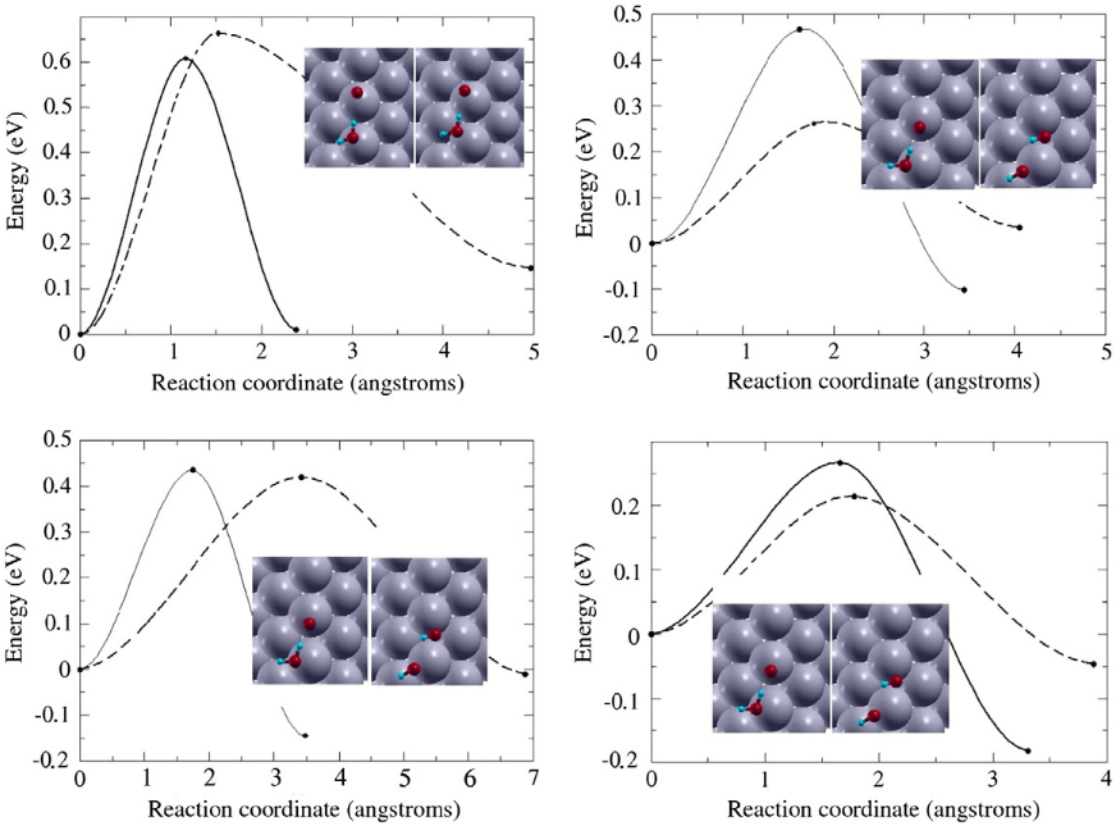

Fig. 6. Activation energy for water dissociation with coadsorbed atomic oxygen assistance following the $H_2O + O \rightarrow OH + OH$ reaction. Relative energy (vertical axis, eV) vs. reaction coordinate (horizontal axis, Å) of the water dissociation minimum energy pathway (MEP) assisted for atomic oxygen. On the left side of every picture, the $H_2O + O$ species as shown on the Fig. 4a, b, c and d. The relative energy is taken as 0 eV in every picture. On the right side, the coadsorption of two OH species after water dissociation, as shown on the Fig. 4f and g. Also shown the configuration of the maximum of every MEP.

between configurations to the activation energy for H_2O dissociation to find that there is no strong preferential configuration for the H_2O molecule to dissociate, although dissociation from configuration *d* seems to be slightly more likely. The activation energy for dissociation from configurations *a* to *f* is about 0.61 eV, whereas the activation energy for dissociation from configurations *b* to *f* is about 0.47 eV. But the energy difference between configurations could be added to obtain 0.58 (0.47 + 0.11) eV. A similar energy is obtained in the case of configuration *c* (0.44 + 0.14 = 0.58 eV) and a smaller energy in the case of configuration *d* (0.27 + 0.20 = 0.47 eV). The activation energies for the H_2O molecule dissociation from configurations *a*, *b*, *c* and *d* to configuration *g* are about 0.66, 0.37, 0.56 and 0.41 eV, respectively. Again, dissociation seems to be slightly more likely from configuration *d* and, in this case, also from configuration *b*. On the other hand, the H_2O molecule can desorb from the surface instead of dissociate. The activation energy for H_2O desorption from the clean surface is the adsorption energy, 0.38 eV, because the activation energy for adsorption is 0 eV. The activation energies for H_2O desorption from configurations *a*, *b*, *c* and *d* are 0.38, 0.31, 0.26 and 0.18 eV, respectively. The interaction energy between the H_2O molecule and the coadsorbed oxygen is about 0 eV in configuration *a*. The repulsive energies are no more than 0.2 eV for the other configurations. For the desorption process, it is also possible to include the energy needed to reach the configurations. For the mentioned configurations, the energies are 0.38, 0.42, 0.40 and 0.38 eV, respectively. These energies are a bit smaller than the energies for H_2O dissociation and the system seems to be dynamic in the two competitive processes of H_2O dissociation and desorption. Diffusion of the adsorbed oxygen atoms seems to be much less likely than diffusion of the H_2O molecule. Probably the activation energy for H_2O diffusion along the *ridge* is about 0.2 eV, which is the energy difference between configurations *a* and *d*.

4. Conclusions

The H_2O adsorption on the clean Pt{110}(1 × 2) surface is an exothermic process with no activation energy, even in the presence of atomic oxygen coadsorbed. On the clean surface, the adsorption energy of the most stable configuration is −0.38 eV. The energy difference between molecular adsorption and dissociative adsorption (OH + H) is at least 0.45 eV and the activation energy for partial dissociation is calculated 0.73 eV. The atomic oxygen coadsorption does not decrease the energy difference (as long as it does not assist the partial dissociation). Due to the activation energy for desorption (0.38 eV) which is about 0.35 eV below the activation energy for dissociation (0.73 eV), the isolated H_2O molecule is likely to desorb from the surface in lieu of dissociate on it. The H_2O partial dissociation, thermodynamically, is not a favorable process on the clean Pt{110}(1 × 2) surface, even in the presence of atomic oxygen on the surface, if it does not assist the dissociation.

On the other hand, the energy difference between the H_2O molecular adsorption and the partial dissociation is decreased if an atomic oxygen takes part of the dissociation process. The dissociation process involves the H_2O and O coadsorption initially and the products are two OH species adsorbed on the surface, without the OH + H + O intermediate step. In these cases the energy difference between molecular adsorption and partial dissociation decreases notably. The dissociation process could be exothermic or endothermic, depending on the initial H_2O + O and final OH + OH energies. There exist several $H_2O + O \rightarrow OH + OH$ reaction pathways in which the energy difference between reactants and products is much smaller than the energy difference between H_2O and OH + H. This would indicate that the oxygen assistance in the H_2O molecular dissociation increases the probability of dissociation.

The activation energies of several $H_2O + O \rightarrow OH + OH$ reactions have been calculated and compared with the calculated desorption energies of the coadsorbed H_2O molecule. The activation energies for dissociation are a bit higher than the activation energies for desorption but there is no strong preference of occurrence of one of the processes over the other one. The comparison shows that dissociation and desorption of coadsorbed H_2O are competitive processes and the system is likely to be dynamic, under the present conditions.

Acknowledgments

This work was supported by Consejo de Investigaciones Científicas y Técnicas (CONICET) PICT 2008 1036 and PIP 0751, Agencia Nacional de Promoción Científica y Tecnológica (ANPCyT) PICT 06 31995, Universidad Nacional de La Plata and the Faculty of Chemistry and Engineering Fray Roger Bacon, Rosario, Argentina.

References

[1] P.A. Thiel, T.E. Madey, Surf. Sci. Rep. 6–8 (1987) 211.
[2] M.A. Henderson, Surf. Sci. Rep. 46 (2002) 1.
[3] A. Verdaguer, G.M. Sacha, H. Bluhm, M. Salmeron, Chem. Rev. 106 (2006) 1478.
[4] T. Mitsui, M.K. Rose, E. Fomin, D.F. Ogletree, M. Salmeron, Science 297 (2002) 1850.
[5] P.J. Feibelman, Science 295 (2002) 99.
[6] S. Volkening, K. Bedurftig, K. Jacobi, J. Wintterlin, G. Ertl, Phys. Rev. Lett. 83 (1999) 2672.
[7] A. Michaelides, P. Hu, J. Am. Chem. Soc. 123 (2001) 4235.
[8] K. Jacobi, K. Bedurftig, Y. Wang, G. Ertl, Surf. Sci. 472 (2001) 9.
[9] A. Michaelides, V.A. Ranea, P.L. de Andrés, D.A. King, Phys. Rev. Lett. 90 (2003) 216102.
[10] H. Ogasawara, B. Brena, D. Nordlund, M. Nyberg, A. Pelmenschikov, L.G.M. Pettersson, A. Nilsson, Phys. Rev. Lett. 89 (2002) 276102.
[11] A. Shavorskiy, M. Gladys, G. Held, Phys. Chem. Chem. Phys. 10 (2008) 6150.
[12] J. Carrasco, A. Michaelides, M. Forster, S. AHaq, R. Raval, A. Hodgson, Nat. Mater. 8 (2009) 427.
[13] E.E. Mola, PhD Thesis, National Universitiy of La Plata, Argentina, 1973.
[14] J. Fusy, R. Ducros, Surf. Sci. 237 (1990) 53.
[15] A. Shavorskiy, T. Eralp, M.J. Gladys, G. Held, J. Phys. Chem. C 113 (2009) 21755.
[16] A. Mondal, H. Seenivasan, A.K. Tiwari, J. Chem. Phys. 137 (2012) 094708.
[17] H. Seenivasan, A.K. Tiwari, J. Chem. Phys. 139 (2013) 174707.
[18] G. Ertl, Surf. Sci. 299 (300) (1994) 742.
[19] A.V. Walker, B. Klötzer, D.A. King, J. Chem. Phys. 109 (1998) 6879.
[20] P. Thostrup, E. Kruse, T. Vestergaard, E. Lægsgaard, F.J. Besenbacher, J. Phys. Chem. B 118 (2003) 3724.
[21] B.L.M. Hendriksen, J.W.M. Frenken, Phys. Rev. Lett. 89 (2002) 046101.
[22] T. Pedersen, W. Li, B. Hammer, Phys. Chem. Chem. Phys. 8 (2006) 1566.
[23] S. Helveg, W.X. Li, N.C. Bartelt, S. Horch, E. Lægsgaard, B. Hammer, F. Besenbacher, Phys. Rev. Lett. 98 (2007) 115501.
[24] W. Moritz, D. Wolf, Surf. Sci. 88 (1979) L29.
[25] D.L. Adams, H.B. Nielsen, M.A. Van Hove, A. Ignatiev, Surf. Sci. 104 (1981) 47.
[26] C.M. Chan, M.A. Van Hove, W.H. Weinberg, E.D. Williams, Solid State Commun. 30 (1979) 47.
[27] R. Koch, M. Borbonus, O. Haase, K.H. Rieder, Appl. Phys. A55 (1992) 417.
[28] J. Carrasco, J. Klimes, A. Michaelides, J. Chem. Phys. 138 (2013) 024708.
[29] A.L. Glebov, A.P. Graham, A. Menzel, Surf. Sci. 427–428 (1999) 22.
[30] S. Timuss, A. Wander, D.A. King, Chem. Rev. 96 (1996) 1291.
[31] F.R. Laffir, V. Fiorin, D.A. King, J. Chem. Phys. 128 (2008) 114717.
[32] T. Panczyk, V. Fiorin, R. Blanco-Alemany, D.A. King, J. Chem. Phys. 131 (2009) 064703.
[33] J. Ren, S. Meng, Phys. Rev. B 77 (2008) 054110.
[34] A. Michaelides, P. Hu, J. Chem. Phys. 114 (2001) 513.
[35] C. Clay, S. Haq, A. Hodgson, Phys. Rev. Lett. 92 (2004) 046102.
[36] W. Lew, M.C. Crowe, C.T. Campbell, J. Carrasco, A. Michaelides, J. Phys. Chem. C 115 (2011) 23008.
[37] G. Kresse, J. Hafner, Phys. Rev. B 49 (1994) 14251.
[38] G. Kresse, J. Furthmuller, Phys. Rev. B 54 (1996) 11169.
[39] P. Blöchl, Phys. Rev. B 50 (1994) 17953.
[40] G. Kresse, D. Joubert, Phys. Rev. B 59 (1999) 1758.
[41] J.P. Perdew, J.A. Chevary, S.H. Vosko, K.A. Jackson, M.R. Pederson, D.J. Singh, C. Fiolhais, Phys. Rev. B 46 (1992) 6671.
[42] G. Henkelman, B.P. Uberuaga, H. Jónsson, J. Chem. Phys. 113 (2000) 9901.
[43] R.W.G. Wyckoff, Crystal Structures, Second edition Interscience, New York, 1965.
[44] S.J. Jenkins, M.A. Petersen, D.A. King, Surf. Sci. 494 (2001) 159.
[45] S.M. Foiles, Surf. Sci. 191 (1987) L779.
[46] E.C. Sowa, M.A. Van Hove, D.L. Adams, Surf. Sci. 199 (1988) 174.
[47] P. Fery, W. Moritz, D. Wolf, Phys. Rev. B 38 (1988) 7275.
[48] E. Vlieg, I.K. Robinson, K. Kern, Surf. Sci. 233 (1990) 248.
[49] J.I. Lee, W. Mannstadt, A.J. Freeman, Phys. Rev. B 59 (1999) 1673.
[50] K.-M. Ho, K.P. Bohnen, Chem. Phys. Lett. 59 (1987) 1833.
[51] A.A. Phatak, W.N. Delgass, F.H. Ribeiro, W.F. Schneider, J. Phys. Chem. C 113 (2009) 7269.
[52] V.A. Ranea, A. Michaelides, R. Ramírez, J.A. Vergés, P.L. de Andrés, D.A. King, Phys. Rev. B 69 (2004) 205411.
[53] V.A. Ranea, J. Chem. Phys. 137 (2012) 204702.
[54] A. Michaelides, V.A. Ranea, P.L. de Andrés, D.A. King, Phys. Rev. B 69 (2004) 075409.
[55] R. Smoluchowski, Phys. Rev. 60 (1941) 661.
[56] Y. Ohno, T. Matsushima, Surf. Sci. 241 (1991) 47.
[57] Y. Ohno, T. Matsushima, S. Tananka, M. Kamada, Jpn. J. Appl. Phys. Suppl. 32–2 (1993) 383.
[58] M.J. Gladys, O.R. Inderwildi, S. Karakatsani, V. Fiorin, G. Held, J. Phys. Chem. C 112 (2008) 6422.